Supplementary Information

Detailed Experimental Procedures

Microarray data and gene filtering

Raw data from all microarrays from Sugino et al. (2006) were imported into R (http://www.r-project.org/), scaled to the same average intensity, and normalized using the quantile normalization method from Bioconductor (http://www.bioconductor.org/) (Bolstad et al., 2003; Choe et al., 2005; Oldham et al., 2006). Presence or absence of probe sets was determined using the MAS 5.0 algorithm. Probe sets were selected based on their consistent presence in at least one cell type and a high coefficient of variation (>0.21), resulting in the selection of 8,000 probe sets. (Note: although some genes are represented by multiple probe sets and other probe sets are not fully annotated, for consistency we refer to probe sets as "genes" and treat them independently throughout this work, unless otherwise noted.) This cohort of 8,000 genes was used to build the network (see below and Oldham et al., 2006). Since genes in modules tend to be highly connected, we selected the most highly connected genes for module detection. The network connectivity (k) for all genes was calculated by summing the connection strengths between each gene and all other genes within the network, then scaling these values to lie between 0 and 1 (Oldham et al., 2006). Genes with a normalized connectivity greater than 0.11 were retained, resulting in a network of 4,097 genes.

Network construction

The network was constructed by calculating the absolute value of the pair-wise Pearson correlations between all genes, raising these correlations to a power, and creating a dissimilarity matrix based on topological overlap, which allows identification of modules of co-expressed genes (Oldham et al., 2006; Ravasz and Barabási, 2003; Zhang and Horvath, 2005). The power that selected to weight the correlations between genes is chosen to recapitulate scale-free topology, as proposed by Zhang and Horvath (2005). We used a power of b=6 for this dataset, which resulted in an approximately scale-

free network (r^2=0.898) and preserved connectivity (mean *k*=52; median *k*=40.8). Modules were created by clustering genes using the average linkage hierarchical clustering algorithm, which has been shown to be useful in analyzing gene expression by placing functionally related genes into groups (Eisen et al., 1998). As the dissimilarity matrix used in hierarchical clustering, we used (1-TO) because TO reflects the relative interconnectedness of two nodes within their local neighborhood, which creates more robust co-expression relationships (Yip and Horvath, 2007).

Module detection and visualization

TO groups entities that share their local neighborhood and, by extension, membership in related functional groups (Barabási and Oltvai, 2004; Horvath et al., 2006; Oldham et al., 2006; Ravasz et al., 2002). We used a combination of dynamic tree cutting algorithms and subsequent evaluation of gene expression to isolate thirteen distinct modules that corresponded to different patterns of gene expression (Horvath et al., 2006; Langfelder et al., 2008). Each module was assigned a color and number to aid in their description. The results of the module detection algorithms were then tested for significance by calculating the average TO within a module and performing permutations using random samples from all genes within the network to generate an empiric p-value (Table I). All of the modules presented here were highly significant ($p < 0.005$), which indicates that each module represents a group of genes that are more likely to be co-expressed than by chance, using TO as a metric of co-expression. Gene expression within modules was visualized by generating standard heat maps with normalized expression values (red denotes high expression, while green denotes low expression).

Modular gene expression

To identify the defining characteristics of each module, singular value decomposition ($X = UDV^T$) was performed and the first principal component (V1) or "module eigengene" was used to summarize the expression profile of a given module. The module eigengene explained a majority of the variance in each module (data not shown). In order to confirm the significance of module characterization, we created indicator vectors for each module, where populations with high expression

values were equal to one and those with low expression values were equal to zero. We then used a Kruskal-Wallis test to compare the module eigengene to the corresponding indicator vector (Oldham et al., 2006).

Module membership

To extend the module definitions to all of the genes on the array platform, we calculated the strength of membership of each gene to each module. As described previously, the expression of each module can be summarized by its first principal component or module eigengene. In order to measure the module eigengene-based module membership (k_{ME}), we calculated the Pearson correlation between the module eigengene and the expression of any gene. A gene that has a high correlation value (high k_{ME}) will have a similar expression pattern to the other genes within the module, and therefore, it is related to the other genes within the module. Due to the fact that k_{ME} is a correlation, each k_{ME} value has a corresponding p-value. Therefore, we calculate k_{ME} and the corresponding p-value for all gene-module combinations to obtain a matrix, describing the membership of each gene to each module. This matrix is used to identify the module or modules to which each gene belongs, which aids in annotation of all genes.

Systematic validation of co-expression relationships

We validated the co-expression relationships on the transcriptional level by obtaining all publicly available microarray data on the MOE430A platform, using the Celsius database that contains ~81,000 Affymetrix microarrays. Data was collected for the top one hundred genes with the highest k_{ME} within each module were obtained, as well as a group of 1,200 random genes. We calculated the mean Pearson correlation between one hundred random genes 1,000 times and calculated the mean and standard deviation for this expected distribution. We then calculated the mean Pearson correlation between all genes within the same module and converted this value to a Z-score using the expected distribution (correlation within module – mean of expected distribution/standard deviation of expected distribution). The Z-score was then converted to a p-value using the cumulative distribution function.

We validated co-expression relationship on the proteomic level by demonstrating that co-expressed genes are more likely to functionally interact. We used a database of protein-protein interactions, and we identified genes within each module that had a k_{ME}>0.7. We calculated an expected distribution for each module by determining the number of interactions that would be expected by chance given the number of genes selected from each module. We then identified the number of protein-protein interactions between genes within the same module and converted this value to a Z-score using the mean and standard deviation of the expected distribution. The Z-score is then converted to a p-value using the cumulative distribution function.

Confirmation of expression with the Allen Brain Atlas

We confirmed the expression of the genes in the black, brown, and midnight blue modules using the Allen Brain Atlas. For each module, we identified genes with a k_{ME} greater than 0.85. The expression of each of these genes was examined in the Allen Brain Atlas (http://www.brainatlas.org/aba/). Different regions of the brain were identified using the atlas that accompanies the *in situ* hybridization data. For the analysis that compared expression in layer V to layer VI, we identified gene expression in layer V of the cortex by comparing the expression to a known marker (*Zfp312*).

***In vivo* validation of network predictions**

Mice with a single large deletion of *Dlx1* and *Dlx2* have been previously characterized (Anderson et al., 1997). *Dlx1*$^{-/-}$/*Dlx2*$^{-/-}$ mutants were identified based on their cleft palate and subsequently by PCR genotyping, but the sex of the specimens was not determined. RNA was purified from the cortex of embryonic day 15.5 wildtype and transgenic animals using Trizol (GibcoBRL). The NINDS/NIMH Microarray Consortium (http://arrayconsortium.tgen.org/np2/home.do) used the purified total RNA to generate biotin-labeled cRNA hybridization probes using the Affymetrix's GeneChip IVT Labeling Kit, which simultaneously performs *in vitro* transcription (a linear ~20-60-fold amplification) and biotin-labeling (see

http://www.affymetrix.com/support/technical/technotes/ivt_technote.pdf). They then performed the amplifications and hybridizations (in duplicate) using the Affymetrix Mouse Genome 430 2.0 array, which has 45,101 probe sets and coverage for 39,000 transcripts. Each expressed gene sequence is represented by 11 probe pairs on the array and each oligonucleotide probe is a 25mer. The arrays were scanned using GeneChip Operating Software (GCOS), which determines the signal intensity of each gene.

The *Rgs4* conditional knockout construct was generated by first cloning a linker into the SacII site of pm30. Pm30 contains a pgk-neo selectable marker flanked by FRT sites and one LoxP site; the linker introduced an additional LoxP site and a unique AvrII site. Next, an 8 kb SpeI restriction enzyme fragment (isolated from BAC RPCI-22-405J3, contains 5' regulatory regions, exon 1 and part of intron 1 (5' homology arm)) was cloned into the AvrII site of pm30 (Supplemental Fig 3). The remainder of exon 1 continuous through the 5' region of exon 5 (4 kb which contains the entire coding sequence except the first 15 amino acids encoded in exon 1) was amplified by PCR, cloned into the SalI site in the region between the LoxP sites of pm30 and then sequenced to confirm the absence of errors (Supplemental Fig 3). Finally, the 3' homology region (3kb including the 3' region of exon 5) was amplified by PCR, cloned into the ApaI site of pm30, and sequenced (Supp Figure 3). The construct was linearized at a unique XhoI site in the vector backbone and electroporated into TL1 (129SvEvTac) cells by the Vanderbilt Transgenic Mouse/ES Cell Shared Resource Core. G418 resistant colonies were selected and genotyped by PCR using primers 5'GAAATTCTCAAAGTGCTAAGA3' and 5'CATTATACGAAGTTATTCGAGG3' (3' domain) and primers 5'CCATTTGAAGCATGACCTGC3' and 5'TGTTCAATGGCCGATCCC3' (5' domain). Long-range PCR was used to verify recombination within the 3' and 5' region (data not shown), and Southern blot was used to confirm homologous recombination using a probe to the 3' homology arm (Supplemental Fig 4a). Blastocyst injection was performed by the Vanderbilt Transgenic Mouse/ES Cell Shared Resource Core, with chimeric founders bred to congenic 129SvEvTac mice to generate a congenic 129-

based *Rgs4* conditional knockout line. Recombinant animals were identified by tail PCR using primers 5'TAACCATGTCCTGTTGGAGC3' and 5'GATGTGGAATGTGTGCGAG3', which spanned a 4.6kb region that was deleted in knockout animals. The PCR reaction included: 1ul DNA, 2.5ul 10X PCR buffer with $MgCl_2$, 2ul dNTP (2.5mM), 0.5ul of each primer, 0.25ul of Amplitaq Gold, and 18.25ul of water. PCR conditions were as follows: 5 minutes at 94°C, followed by 35 cycles that included, 30 seconds at 94°C, 30 seconds at 60°C, and 1 minute at 72°C, and finally an extension step of 10 minutes at 72°C. In the knockout animals, this reaction yielded a product of 644bp. A constitutive *Rgs4* knockout line was generated by breeding to a 129-congenic protamine-CRE (general deletor) line (www.jax.org, stock # 3328). Heterozygous constitutive nulls were intercrossed to generate control and knockout tissue for microarrays and to confirm loss of *Rgs4* at the protein level. Western blots were performed using protein isolated from three strains of adult mouse frontal cortex, including wild-type mice, mice that over-express *Rgs4* (Ding et al., 2006), and *Rgs4* knockout mice. A polyclonal antibody to *Rgs4* (rabbit anti-*Rgs4*, a kind gift of Dr. Suzanne Mumby, UT Southwestern Medical Center at Dallas) was used at a dilution of 1:2000 (Supplemental Fig 4c). Total RNA was obtained from the frontal cortex of four *Rgs4* knockout adult animals and four wildtype adult animals. Microarrays were performed on Affymetrix MOE430A platform with 22,690 probe sets.

Probe set level data were obtained for all arrays and normalization was performed as described above. We analyzed differential expression between both mutants and wildtype using the data described above. A Bayesian ANOVA (Baldi and Long, 2001) was used to determine differential expression. Differentially expressed genes ($p<0.01$) were counted within each module, and the chi-squared test was used to determine significance. To assess whether connectivity within the module itself also has an effect on differential expression, genes were ranked based on their TO with the gene that was deleted. This list was broken into quartiles and the number of differentially expressed genes ($p<0.01$) for each quartile was counted. The number of differentially expressed genes is expressed as a percentage of the total number of differentially expressed genes. Significance was calculated by

dividing the difference between two percentages by the standard error of the difference and then converting to a p-value.

References

Anderson, S.A., Qiu, M., Bulfone, A., Eisenstat, D.D., Meneses, J., Pedersen, R. and Rubenstein, J.L. (1997). Mutations of the homeobox genes Dlx-1 and Dlx-2 disrupt the striatal subventricular zone and differentiation of late born striatal neurons.. Neuron *19*, 27-37.

Baldi, P. and Long, A.D. (2001). A Bayesian framework for the analysis of microarray expression data: regularized t -test and statistical inferences of gene changes.. Bioinformatics *17*, 509-519.

Barabási, A. and Oltvai, Z.N. (2004). Network biology: understanding the cell's functional organization.. Nat Rev Genet *5*, 101-113.

Bolstad, B.M., Irizarry, R.A., Astrand, M. and Speed, T.P. (2003). A comparison of normalization methods for high density oligonucleotide array data based on variance and bias.. Bioinformatics *19*, 185-193.

Choe, S.E., Boutros, M., Michelson, A.M., Church, G.M. and Halfon, M.S. (2005). Preferred analysis methods for Affymetrix GeneChips revealed by a wholly defined control dataset.. Genome Biol *6*, R16.

Ding, J., Guzman, JN., Tkatch, T. et al. (2006). Rgs4-dependent attenuation of m4 autoreceptor function in striatal cholinergic interneurons following dopamine depletion. *Nat. Neurosci.* **9**: 832-842.

Dong, J. and Horvath, S. (2007). Understanding network concepts in modules.. BMC Syst Biol *1*, 24.

Eisen, M.B., Spellman, P.T., Brown, P.O. and Botstein, D. (1998). Cluster analysis and display of genome-wide expression patterns.. Proc Natl Acad Sci U S A *95*, 14863-14868.

Horvath, S., Zhang, B., Carlson, M., Lu, K.V., Zhu, S., Felciano, R.M., Laurance, M.F., Zhao, W., Qi, S., Chen, Z., et al. (2006). Analysis of oncogenic signaling networks in glioblastoma identifies ASPM as a molecular target.. Proc Natl Acad Sci U S A *103*, 17402-17407.

Langfelder, P., Zhang, B. and Horvath, S. (2008). Defining clusters from a hierarchical cluster tree: the dynamic tree cut package for r. *Bioinformatics* **24**: 719-720.

Li, A. and Horvath, S. (2007). Network neighborhood analysis with the multi-node topological overlap measure.. Bioinformatics *23*, 222-231.

Oldham, M.C., Horvath, S. and Geschwind, D.H. (2006). Conservation and evolution of gene coexpression networks in human and chimpanzee brains.. Proc Natl Acad Sci U S A *103*, 17973-17978.

Ravasz, E., Somera, A.L., Mongru, D.A., Oltvai, Z.N. and Barabási, A.L. (2002). Hierarchical organization of modularity in metabolic networks.. Science *297*, 1551-1555.

Yip, A.M. and Horvath, S. (2007). Gene network interconnectedness and the generalized topological overlap measure.. BMC Bioinformatics *8*, 22.

Zhang, B. and Horvath, S. (2005). A general framework for weighted gene co-expression network analysis.. Stat Appl Genet Mol Biol *4*, Article17.

Supplemental Figures

a) Summary of neuronal sub-types

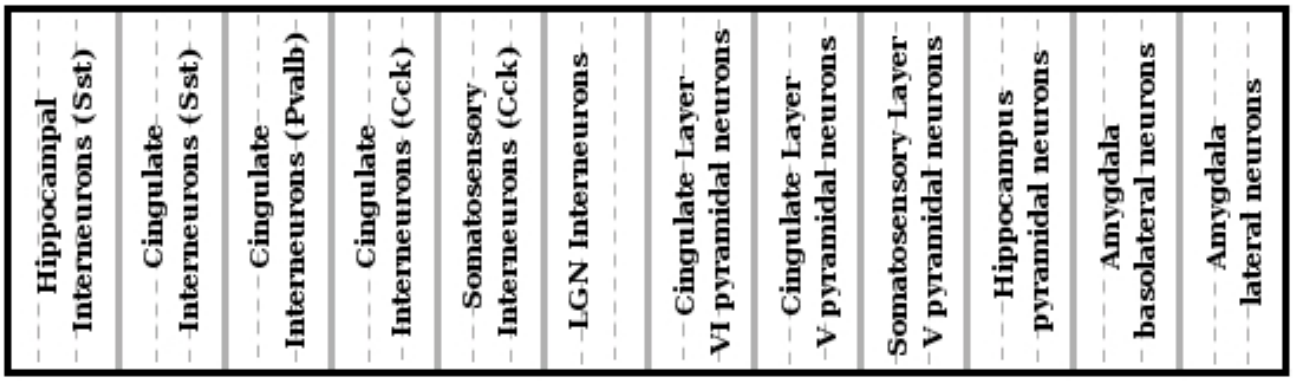

b) Black (#1)

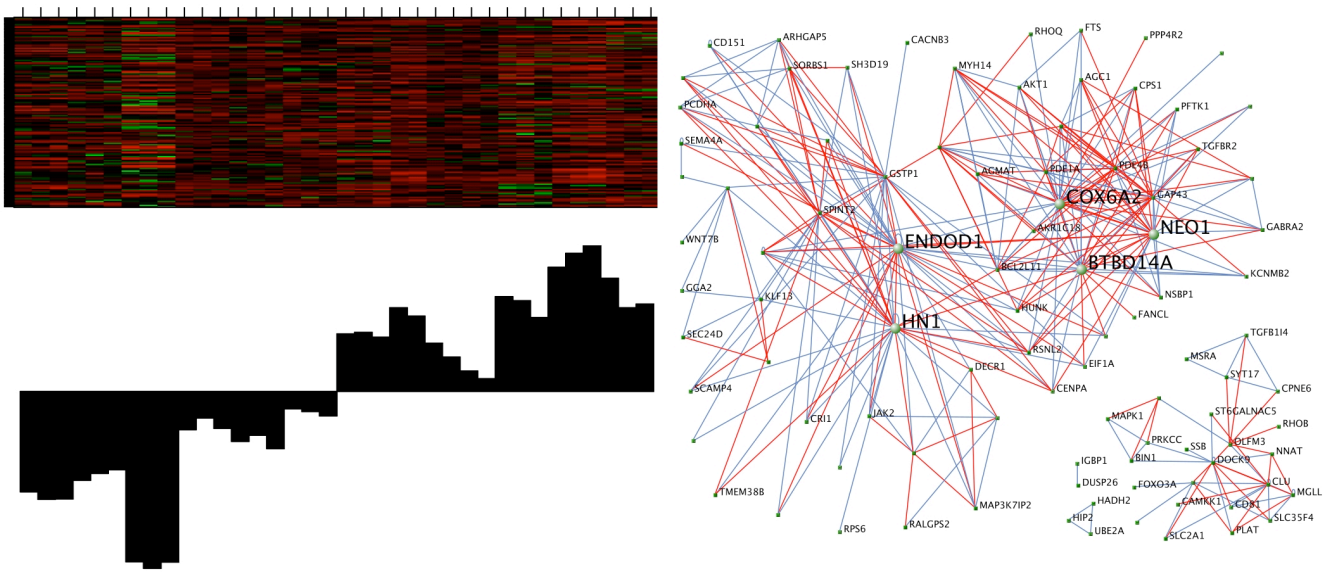

c) Blue (#2)

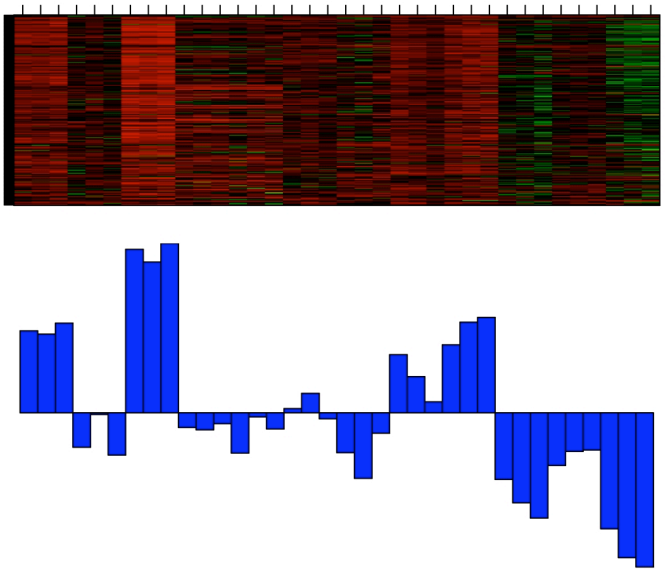

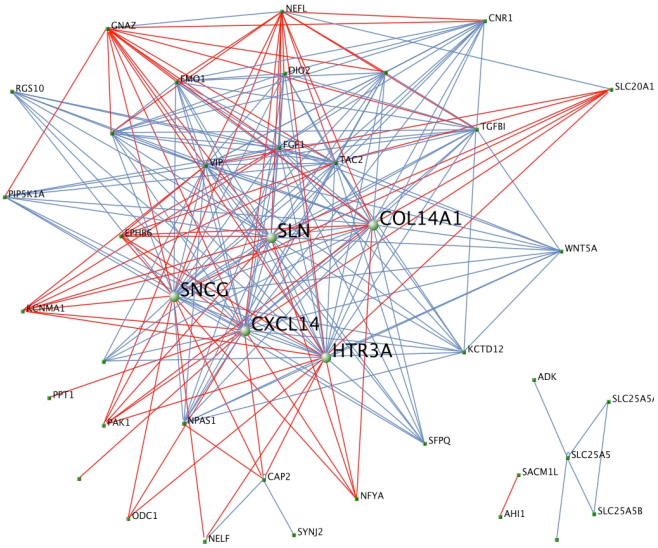

d) Brown (#3)

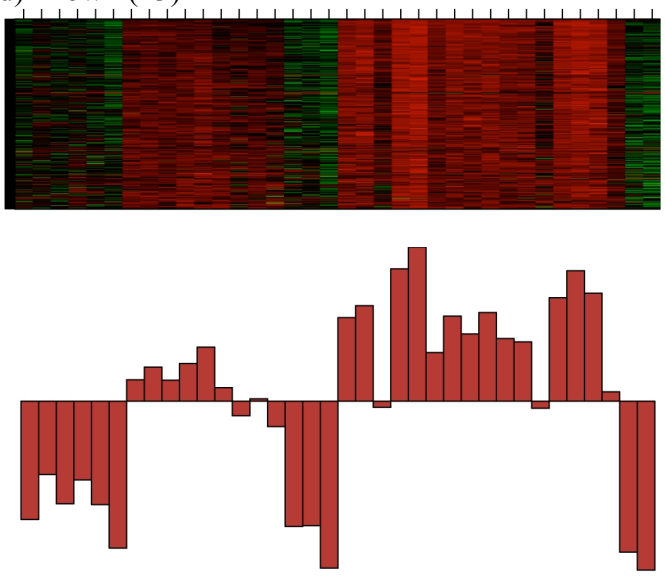

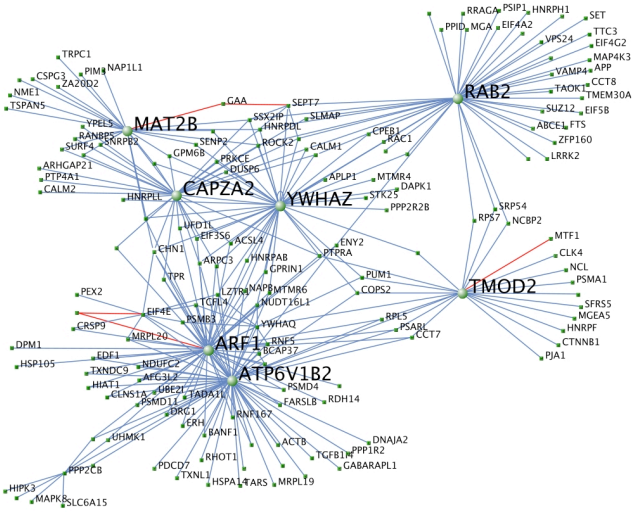

e) Green (#4)

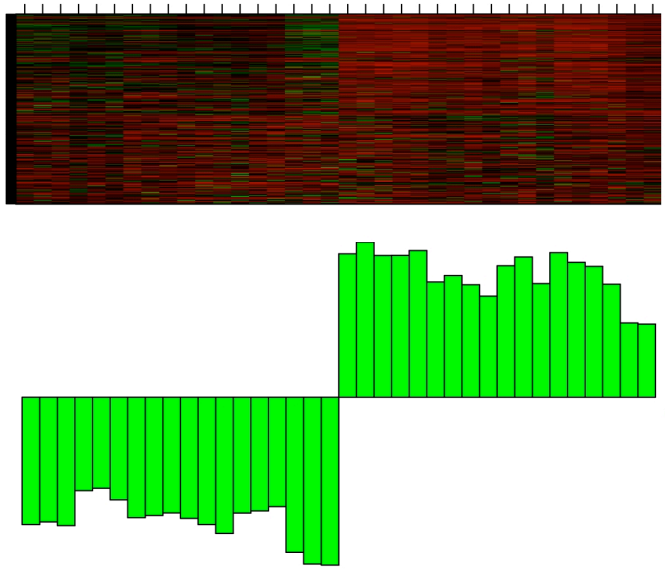

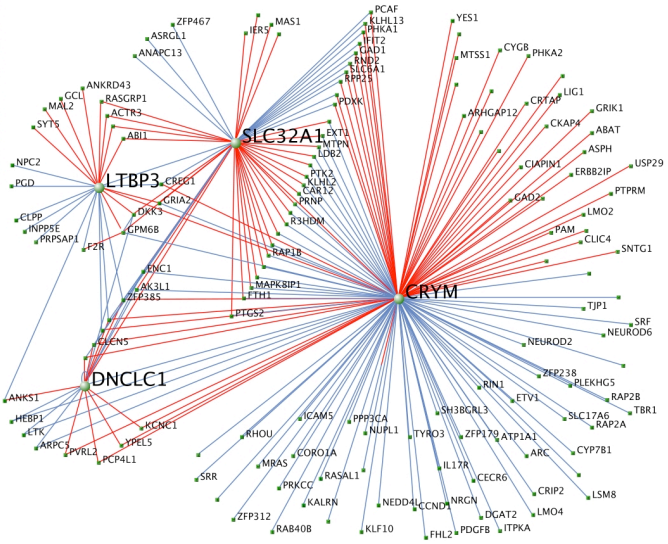

f) Green yellow (#5)

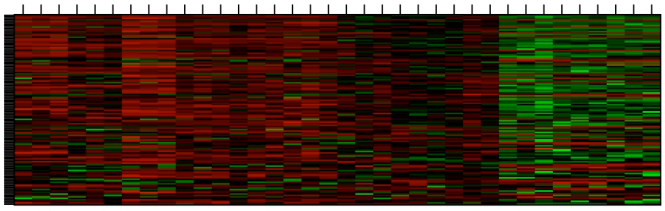

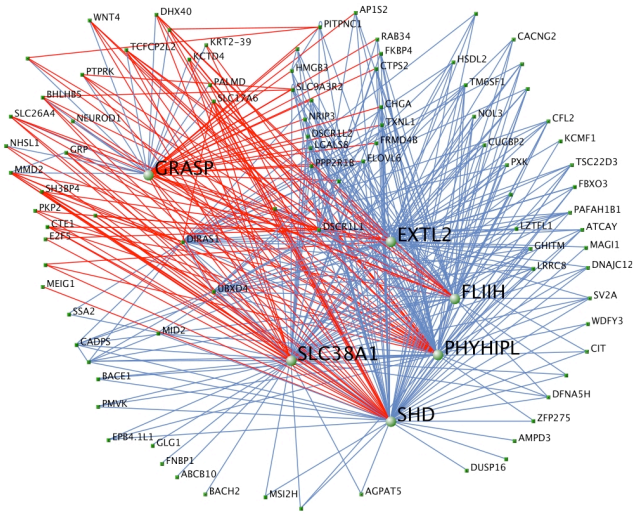

g) Light yellow (#6)

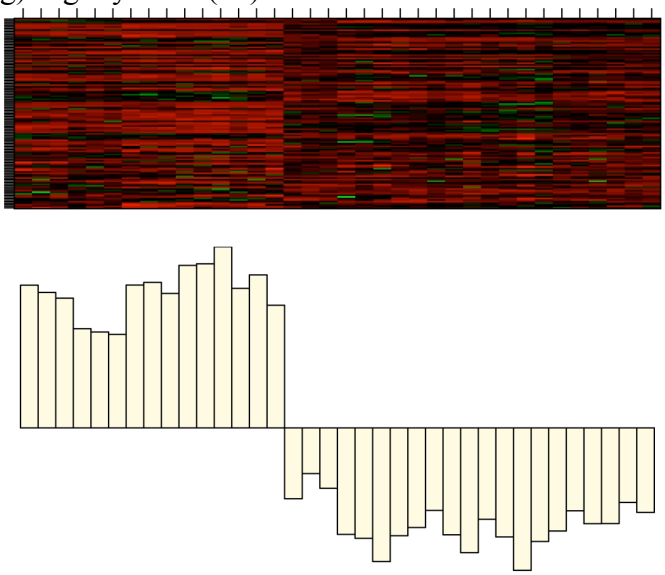

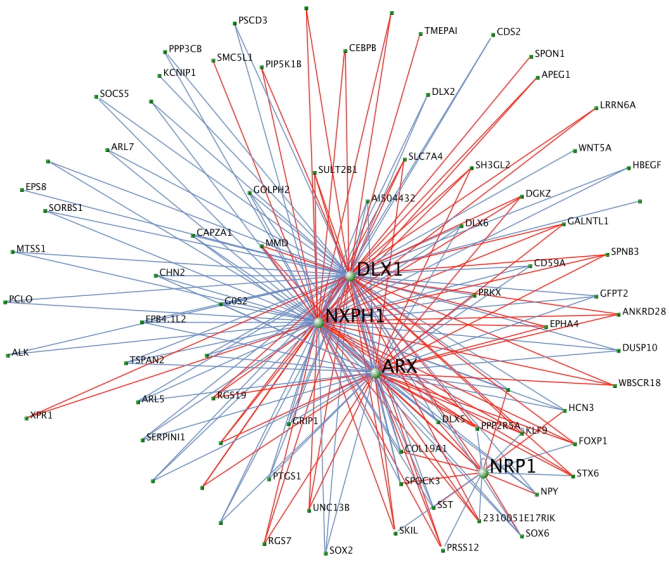

h) Midnight blue (#7)

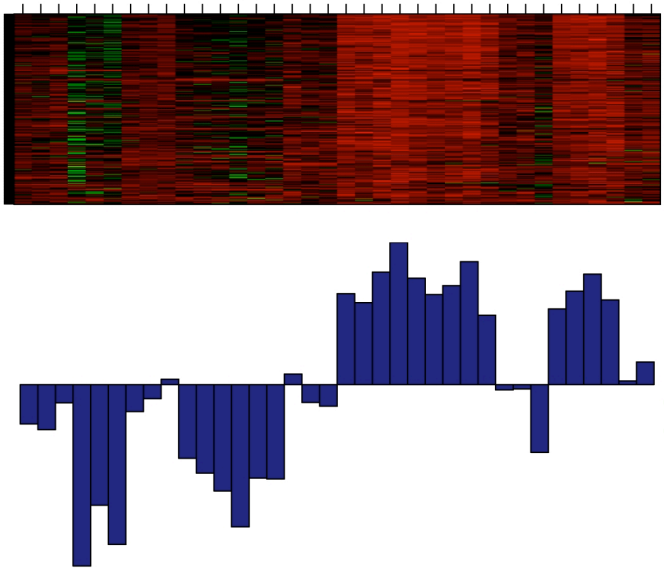

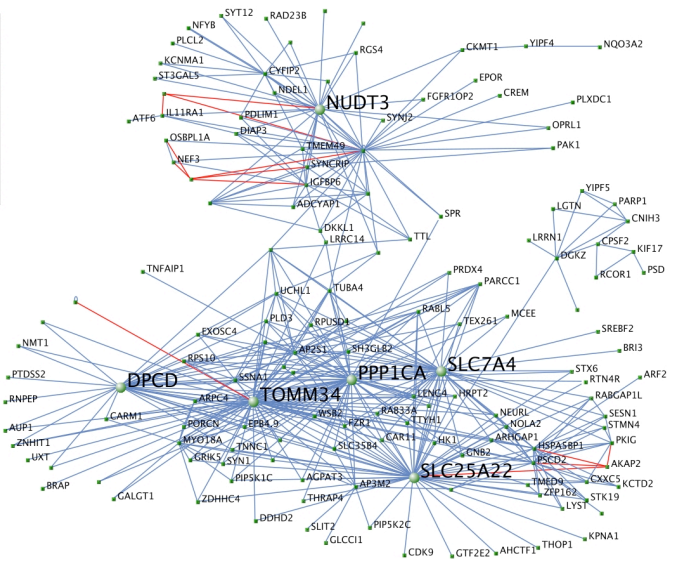

i) Orange (#8)

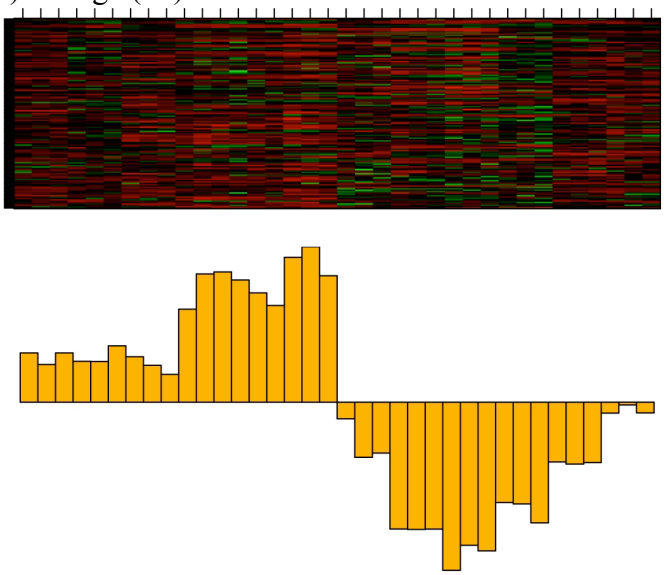

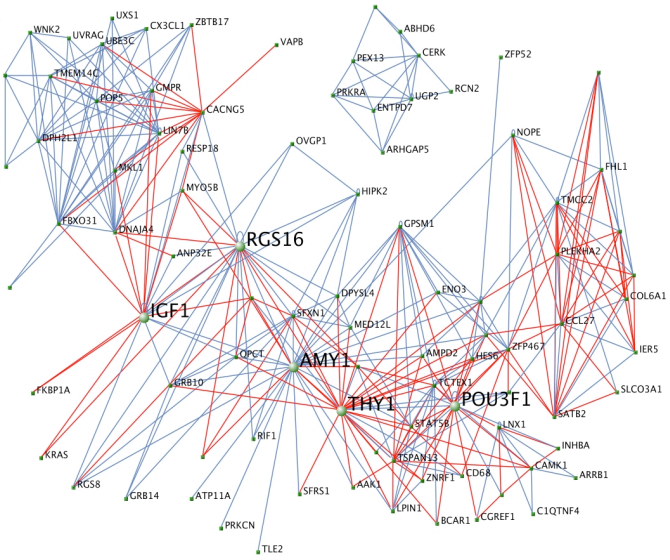

j) Pink (#9)

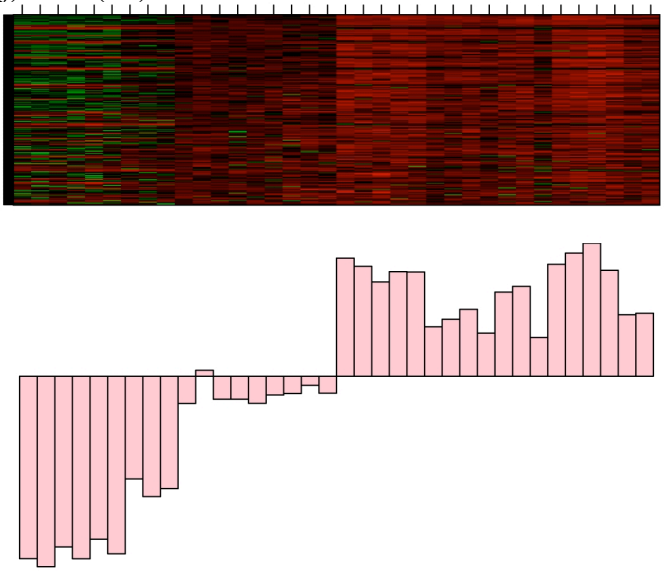

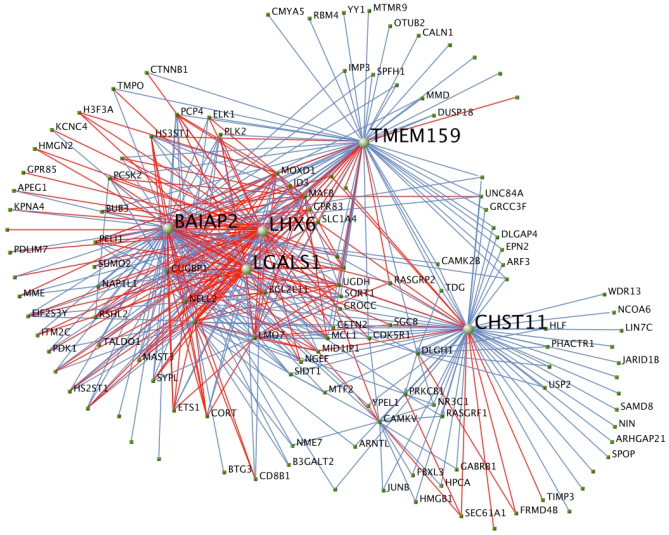

k) Purple (#10)

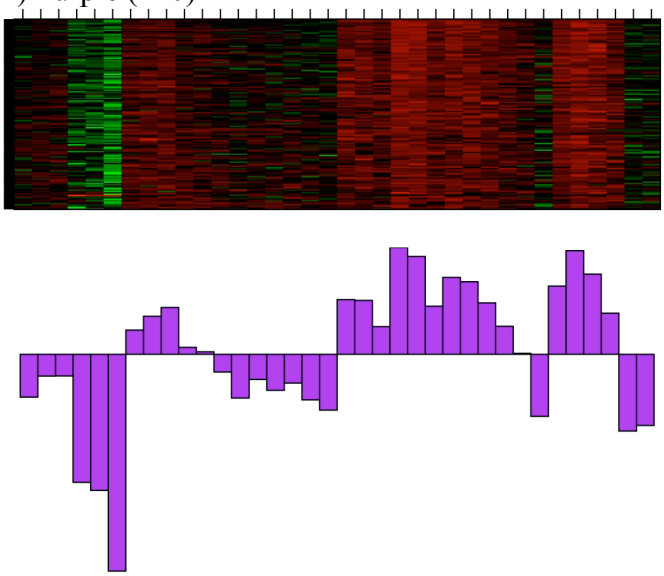

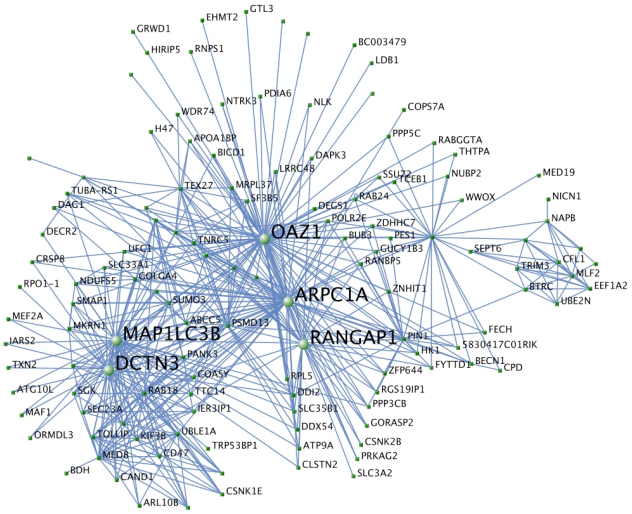

l) Red (#11)

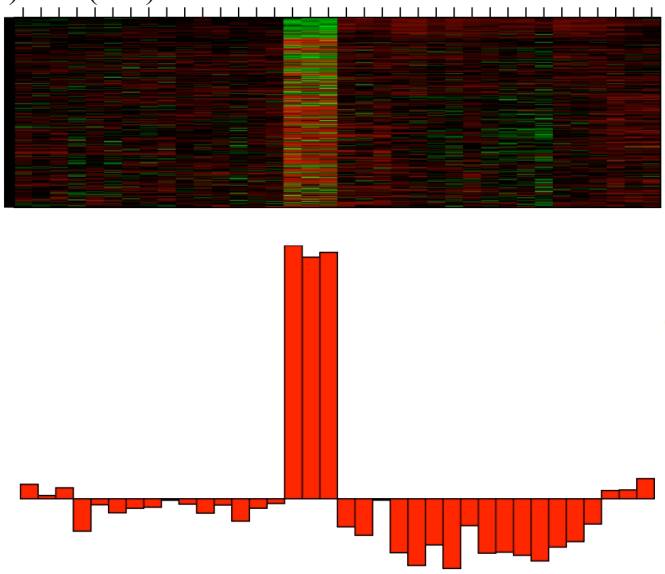

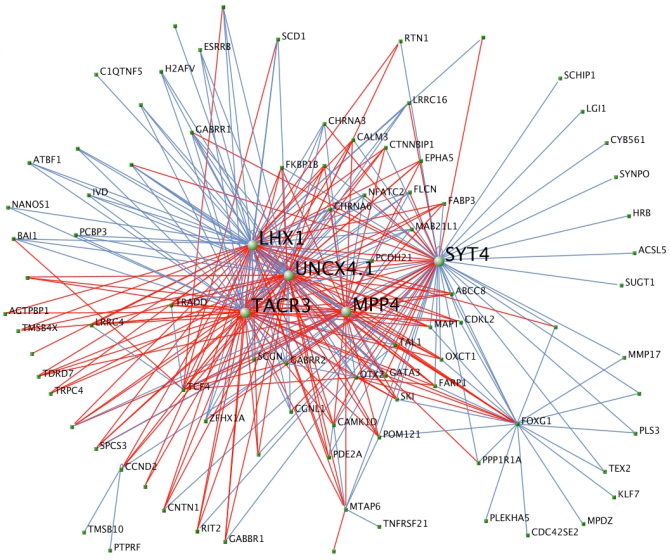

m) Turquoise (#12)

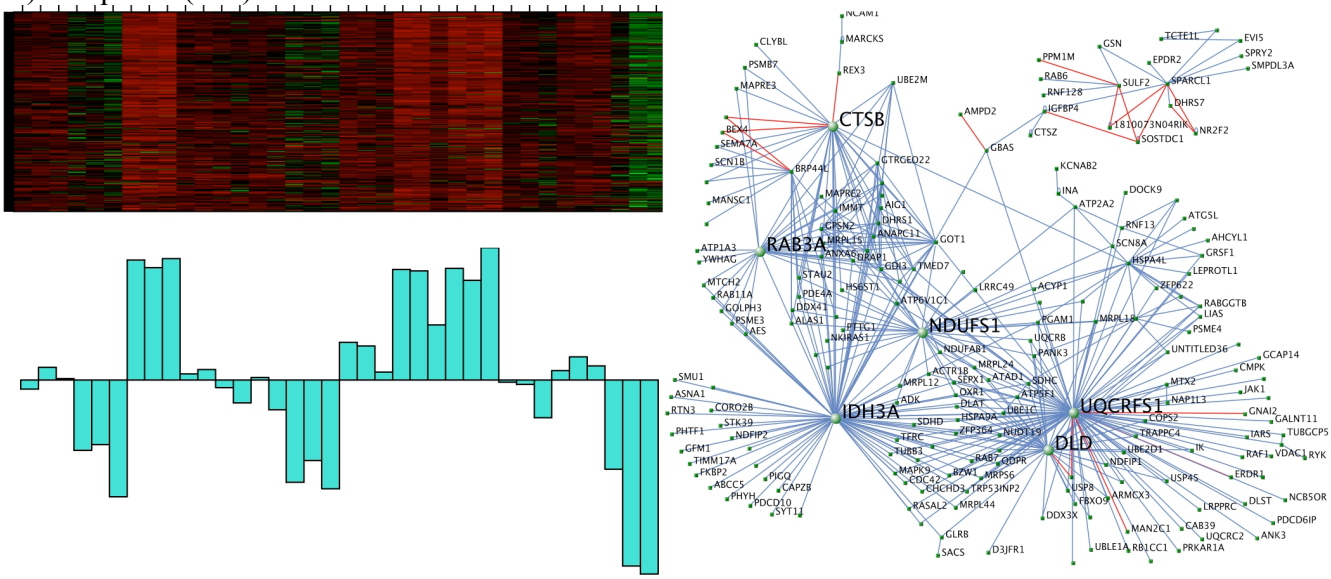

n) Yellow (#13)

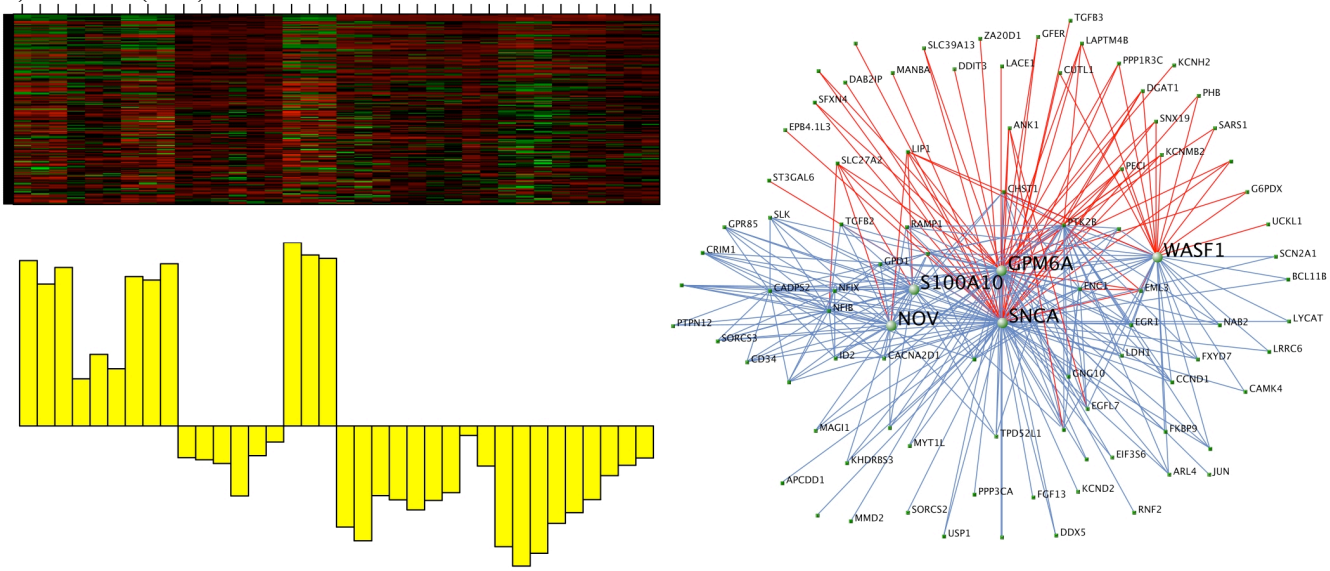

Supplemental Figure 1: Gene expression patterns within modules – Heat maps depicting expression of genes (rows) across all samples (columns) are shown for all modules. Within the heat map, red corresponds to high expression, whereas green corresponds to genes that are expressed at a low level. Below each heat map, a barplot of the module eigengene (ie. first principal component) derived from singular value decomposition summarizes gene expression within the module. a) A map of the different neuronal sub-types across the heat maps is located in the upper left. b) The black (#1) module contains 144 genes and corresponds to hippocampal, basolateral amygdala, and lateral amygdala

pyramidal neurons. The network plot to the right displays the top three hundred connections within the module. c) The blue (#2) module contains 252 genes and corresponds hippocampal somatostatin-positive and cingulate parvalbumin interneurons, as well as layer 5 somatosensory pyramidal neurons. d) The brown (#3) module contains 342 genes and corresponds to layer 5 & 6 cingulate, layer 5 somatosensory, hippocampal, and basolateral amygdala pyramidal neurons . e) The green (#4) module contains 419 genes and corresponds to all excitatory neurons. f) The green yellow (#5) modules contains 130 genes and corresponds to all inhibitory neurons. g) The light yellow (#6) module contains 121 genes and corresponds to inhibitory interneurons derived from the telencephalon. h) The midnight blue (#7) module contains 234 genes and corresponds to layer 5 &6 cingulate, layer 5 somatosensory, and basolateral amygdala pyramidal neurons. i) The orange (#8) module contains 139 genes and corresponds to cingulate cholecystokinin-positive, somatosensory cholecystokinin-positive, and LGN interneurons. j) The pink (#9) module contains 249 genes and corresponds to all excitatory neurons. k) The purple (#10) module contains 143 genes and corresponds to layer 5 & 6 cingulate, layer 5 somatosensory, and basolateral amygdala pyramidal neurons. l) The red (#11) module contains 263 genes and corresponds to LGN interneurons. m) The turquoise (#12) module contains 358 genes and corresponds to cingulate parvalbumin-positive interneurons, as well as layer 5 cingulate and layer 5 somatosensory pyramidal neurons. n) The yellow (#13) module contains 189 genes and corresponds to hippocampal somatostatin-positive, cingulate parvalbumin-positive, and LGN interneurons.

a)

Relationship between modules and mean firing rate

Module	Correlation	P-value
Black (#1)	-0.66	0.00001
Blue (#3)	0.62	0.00006
Yellow (#13)	0.60	0.00010
Pink(#9)	-0.57	0.00027
Green yellow (#5)	0.44	0.00665
Light yellow (#6)	0.43	0.00855
Green (#4)	-0.35	0.03729
Turquoise (#12)	0.27	0.11770

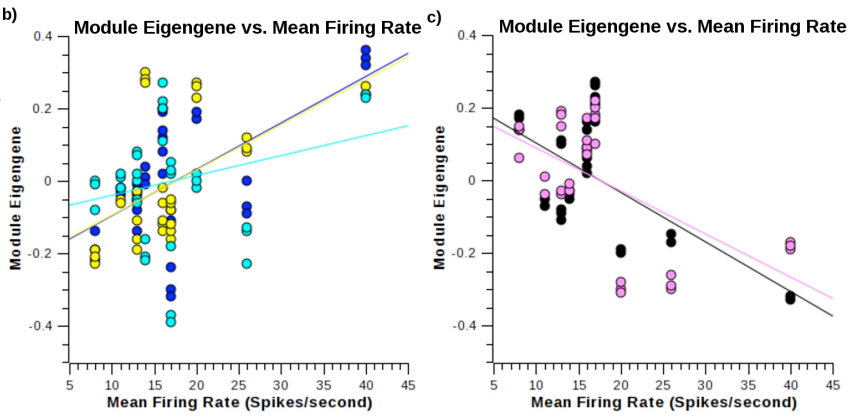

Supplemental Figure 2: Modules correspond to firing rate – Mean firing rate of each cell type was derived from current clamp data presented in Sugino et al., (2006) Figure 1 (see Methods). Firing rate was compared to each module eigengene using a Pearson correlation to assess whether any modules were related to physiological activity. a) Summary of the Pearson correlation and p-value for each comparison of module eigengene and firing rate. Only the data from modules that had nominally significant correlations ($p<0.05$) with firing rate and the turquoise module are shown. Of these, four modules showed significant correlation with firing rate after Bonferroni correction (Blue (#2), Yellow (#13), Pink (#9), and Black (#1)), while the other modules did not. b) This scatter plot shows the relationship of firing rate to the module eigengenes for the blue (#2), yellow (#13), and turquoise (#12) modules. The blue (#2) and yellow (#13) module eigengenes are significantly positively correlated with firing rate (p=6.2e-5 & 1.0e-4), but the turquoise (#12) module is not (p=0.12). c) This scatter plot shows that the pink (#9) and black (#1) module eigengenes are significantly inversely correlated with firing rate (p=2.7e-5 & p=1.0e-6).

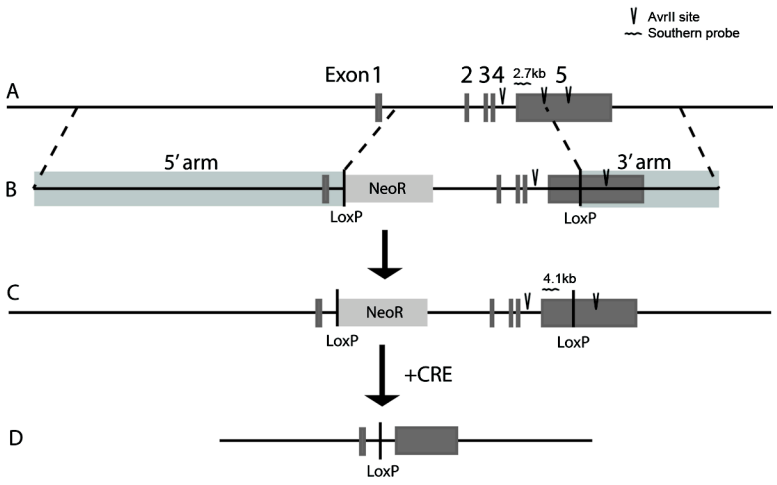

Supplemental Figure 3: Construction of *Rgs4* targeting vector – A schematic describing the targeting vector used to create the *Rgs4* knockout mouse. a) Genomic structure of *Rgs4*. The *Rgs4* coding sequence extends across all 5 transcribed exons, spanning approximately 10 kb. b) *Rgs4* conditional knockout targeting construct. The *Rgs4* KO construct introduces a LoxP site and an FRT-flanked neomycin-resistance cassette into intron 1 of the *Rgs4* gene as well as a LoxP site into the middle of exon 5 (FRT sites are removed for simplicity in this figure). This effectively excises all but the first 15 amino acids of *Rgs4* (encoded by exon 1). c) *Rgs4* conditional knockout construct integrated into the *Rgs4* genomic locus. d) *Rgs4* locus after mouse is mated to a CRE-expressing mouse. Exons 2-4 and the 5' region of exon 5 are removed, leaving only exon 1 and the 3' region of exon 5. The AvrII sites and southern probe were used to confirm homologous recombination at the 3' end, which is described in detail in Supplemental Figure 4.

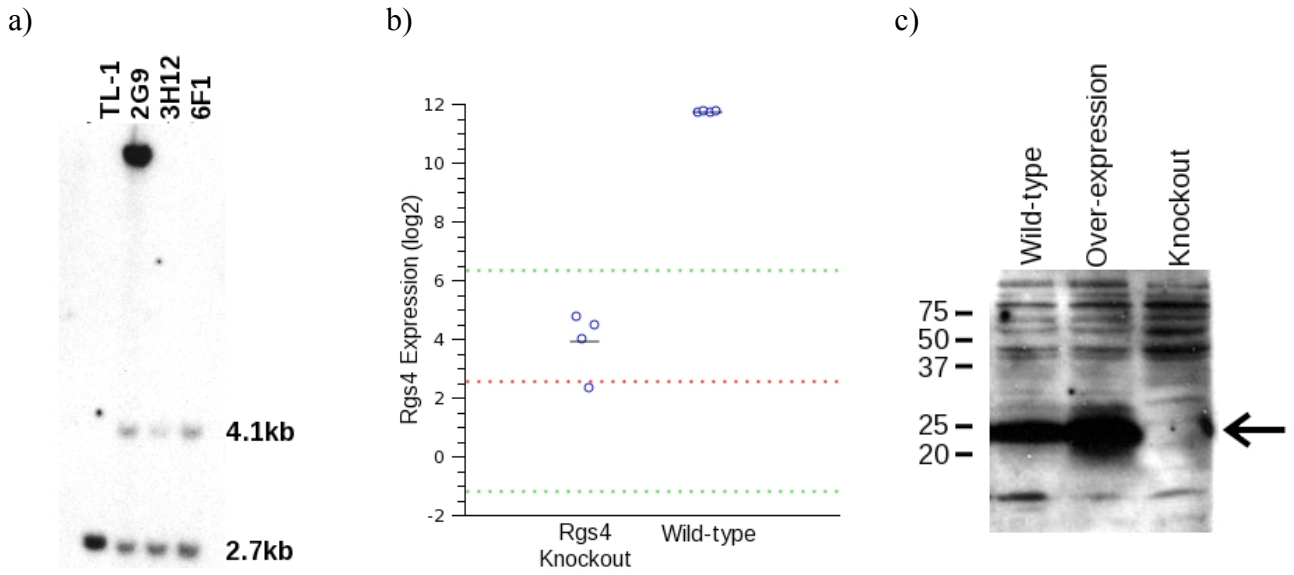

Supplemental Figure 4: Confirmation of *Rgs4* deletion – Verification of disruption of *Rgs4* on the DNA, mRNA, and protein levels. a) Homologous recombination of the targeting vector in the 3' homology region was verified by Southern blot. TL-1 represents the parent stem cell line that was used for the *Rgs4* targeting event, and 2G9, 3H12, and 6F1 were the only clones obtained after injection of the targeting vector and selection with G418. The *Rgs4* locus has two AvrII sites, immediately 5' and 3' to the 3' homology arm (see Supplemental Fig 3), but the 3' AvrII site was mutated during the introduction of the LoxP site. The probe is located 3' of the 3' AvrII site, and therefore, the parent cell line only shows a smaller band at 2.7kb, which demonstrates that the 3' AvrII site is intact. In all three clones (2G9, 3H12, and 6F1), we observed a larger band at 4.1kb, which shows that the 3' AvrII site is absent but the 5' AvrII site is present, confirming the presence of the second LoxP site because it is located between these restriction sites. Clone 2G9 had additional insertions evidenced by the large band at the top, and therefore, we used clone 3H12 for the generation of transgenic mice. b) Microarray data showing the expression of *Rgs4* in the knockout and wild-type frontal cortex. The blue circles show the individual data points for *Rgs4* expression, and the black horizontal bar denotes the mean expression. The red dashed line displays the mean expression for all absent genes, and the green

dashed line shows two standard deviations of expression for all absent genes. *Rgs4* is highly expressed in the wild-type mice, but expression values are similar to genes that are called absent in the knockout animals, further confirming disruption of *Rgs4*. c) Western blot of protein extracts from frontal cortex of wild-type mice, mice that over-express *Rgs4* (Ding et al., 2006), and knockout mice of *Rgs4* using an anti-*Rgs4* antibody (see Supplemental Methods). *Rgs4* is a 24kDa protein, and the arrow denotes position of *Rgs4* protein in the wild-type and over-expression mice. Note the absence of *Rgs4* protein in the knockout strain.

Supplemental Tables

Supplemental Table 1 - Summary of all neuronal classes used in the analysis

Array	Tissue	Neuro-transmitter	Peptide/ Location	Strain	Average correlation	Standard deviation
GSM63015	Hippocampus	GABA		GIN	0.911	0.021
GSM63016	Hippocampus	GABA		GIN	0.912	0.021
GSM63017	Hippocampus	GABA		GIN	0.914	0.021
GSM63018	Cingulate	GABA	Sst	GIN	0.897	0.021
GSM63019	Cingulate	GABA	Sst	GIN	0.907	0.020
GSM63020	Cingulate	GABA	Sst	GIN	0.900	0.021
GSM63021	Cingulate	GABA	Pvalb	G42	0.915	0.020
GSM63022	Cingulate	GABA	Pvalb	G42	0.912	0.020
GSM63023	Cingulate	GABA	Pvalb	G42	0.915	0.020
GSM63024	Cingulate	GABA	Cck	G30	0.917	0.018
GSM63025	Cingulate	GABA	Cck	G30	0.912	0.020
GSM63026	Cingulate	GABA	Cck	G30	0.915	0.019
GSM63027	Somatosensory	GABA	Cck	G30	0.905	0.020
GSM63028	Somatosensory	GABA	Cck	G30	0.918	0.018
GSM63029	Somatosensory	GABA	Cck	G30	0.911	0.019
GSM63030	LGN	GABA		G42	0.901	0.021
GSM63031	LGN	GABA		G42	0.903	0.021
GSM63032	LGN	GABA		G42	0.899	0.022
GSM63033	Cingulate	Glutamate	Layer VI	C57/Bl6	0.915	0.021
GSM63034	Cingulate	Glutamate	Layer VI	C57/Bl6	0.912	0.022
GSM63035	Cingulate	Glutamate	Layer VI	C57/Bl6	0.915	0.020
GSM63036	Cingulate	Glutamate	Layer V	YFPH	0.923	0.024
GSM63037	Cingulate	Glutamate	Layer V	YFPH	0.923	0.024
GSM63038	Cingulate	Glutamate	Layer V	YFPH	0.920	0.022
GSM63039	Somatosensory	Glutamate	Layer V	YFPH	0.915	0.024
GSM63040	Somatosensory	Glutamate	Layer V	YFPH	0.917	0.021
GSM63041	Somatosensory	Glutamate	Layer V	YFPH	0.916	0.022
GSM63042	Hippocampus	Glutamate		YFPH	0.916	0.024
GSM63043	Hippocampus	Glutamate		YFPH	0.911	0.024
GSM63044	Hippocampus	Glutamate		YFPH	0.905	0.024
GSM63045	Amygdala	Glutamate	Basolateral	YFPH	0.920	0.024
GSM63046	Amygdala	Glutamate	Basolateral	YFPH	0.920	0.024
GSM63047	Amygdala	Glutamate	Basolateral	YFPH	0.920	0.024
GSM63048	Amygdala	Glutamate	Lateral	G30	0.913	0.021
GSM63049	Amygdala	Glutamate	Lateral	G30	0.908	0.020
GSM63050	Amygdala	Glutamate	Lateral	G30	0.906	0.020

This table summarizes the different classes of neurons, which were included in the analysis. The first column corresponds to the array names from Geo DataSets. The tissue describes where the neurons were obtained from, and the neurotransmitter column describes the main neurotransmitter of the isolated neurons. The peptide/location column describes a distinguishing characteristic, which differentiates it from the rest of the populations. The strain corresponds to the mouse strain that the neurons were obtained from. The average correlation and standard deviation describe the correlations with all of the other arrays in the data set.

Supplemental Table 2 - Summary of GO analysis for each module

Module	Biological Process	Cellular Compartment	Molecular Function
Black (#1)	-Cellular protein metabolism (p=0.0012) -Small GTPase mediated signal transduction (p=0.0041) -Protein transport (p=0.029)	-Chromatin (p=0.017) -Chromosome (p=0.049)	-Protein kinase activity (p=0.016) -GTP binding (p=0.017) -Sugar porter activity (p=0.021)
Blue (#2)	-Carboxylic acid metabolism (p=1.2e-4) -Cellular carbohydrate metabolism (p=0.0036) -Electron transport (p=0.0048)	-Mitochondrion (p=1.86e-6)	-Voltage-gated channel activity (p=0.0015) -FGF receptor binding (p=0.0022) -Hyaluronic acid binding (p=0.015)
Brown (#3)	-Protein transport (p=2.1e-6) -Establishment of cellular localization (p=2.8e-4) -RNA metabolism (p=0.0016)	-Nucleus (p=4.6e-4) -Spliceosome complex (p=0.036)	-ATP binding (p=1.3e-4) -Ubiquitin-protein ligase activity (p=2.6e-3) -Protein kinase activity (p=0.012)
Green(#4)	-Synaptic transmission (p=3.7e-4) -Axon guidance (p=0.0084) -Neuron differentiation (p=0.011)	-Cytoskeleton (p=0.021)	-GTP binding (p=4.1e-4) -Protein kinase activity (p=0.026)
Green yellow (#5)	-Oogenesis (p=0.063) -Neuroblast proliferation (p=0.078)	-Cytoskeleton (p=0.063)	-ATP binding (p=0.084)
Light yellow (#6)	-Synaptic vesicle transport (p=0.0053) -Cell migration (p=0.026) -Neuron differentiation (p=0.031)	-Transcription factor complex (p=0.069) -Actin cytoskeleton (p=0.079)	-Potassium ion binding (p=0.078)
Midnight blue (#7)	-Intracellular transport (p=0.0041) -Neuron morphogenesis during differentiation (p=0.0053) -Cytoskeleton-dependent intracellular transport (p=0.0066)	-Coated vesicle (p=0.0035) -Golgi apparatus (p=0.034)	-GTP binding (p=0.054) -Acyltransferase activity (p=0.089)
Orange (#8)	-Apoptosis (p=0.009) -Negative regulation of axonogenesis (p=0.046) -Neuron differentiation (p=0.052)		-Protein kinase activity (p=0.021) -ATP binding (p=0.093)
Pink (#9)	-Small GTPase mediated signal transduction (p=0.0085) -Protein transport (p=0.0098) -Transcription (p=0.015)	-Nucleus (p=0.02) -Golgi stack (p=0.04)	-Protein kinase activity (p=0.0029) -Protein histidine kinase activity (p=0.033)
Purple (#10)	-Wnt receptor signaling pathway (p=0.0038) -Cellular protein metabolism (p=0.011) -Ribosome biogenesis and assembly (p=0.035)	-Endoplasmic reticulum (p=0.0091) -Signalosome complex (p=0.08)	-GTP binding (p=0.037) -ATP binding (p=0.053)
Red (#11)	-Lipid biosynthesis (p=0.0054) -Negative regulation of programmed cell death (p=0.039) -Synaptic transmission (p=0.076)	-Nuclear chromosome (p=0.064) -Microtubule cytoskeleton (p=0.01)	-GABA-A receptor activity (p=0.005) -Zinc ion binding (p=0.034)
Turquoise (#12)	-Cellular carbohydrate metabolism (p=4.5e-4) -Cell projection biogenesis (p=0.019) -Synaptic transmission (p=0.026)	-Mitochondrion (p=2.5e-11) -Microtubule cytoskeleton (p=0.01)	-ATPase activity (p=0.014) -GTP binding (p=0.021)
Yellow (#13)	-Ion transport (p=5.7e-4) -Nucleocytoplasmic transport (p=0.012) -Nucleobase, nucleoside, and nucleotide transport (p=0.038)	-Lytic vacuole (p=0.043)	-Voltage-gated channel activity (p=0.029) -Protein kinase activity (p=0.035)

This table summarizes selected GO categories for each module. The columns represent categories in biological process, cellular compartment, and molecular function. Only level five GO categories were used. Terms were selected on the basis of uniqueness and over-representation, but each category was limited to maximum three terms per module.

Supplemental Table 3 - Summary of the modules and their significance

Module Eigengene	Corresponding Cell Types
Black (#1)	Hippocampal, Basolateral amygdala, and Lateral Amygdala pyramidal neurons
Blue (#2)	Hippocampal (Sst+) and Cingulate (Pvalb+) interneurons; Somatosensory (Layer 5) pyramidal neurons
Brown (#3)	Cingulate (Layer 5 & 6), Somatosensory (Layer 5), Hippocampal, and Basolateral amygdala pyramidal neurons
Green (#4)	Cingulate (Layer 5 & 6), Somatosensory (Layer 5), Hippocampal, Basolateral amygdala, and Lateral amygdala pyramidal neurons
Green yellow (#5)	Hippocampal (Sst+), Cingulate (Pvalb+/Sst+/Cck+), Somatosensory (Cck+) and LGN interneurons
Light yellow (#6)	Hippocampal (Sst+), Cingulate (Pvalb+/Sst+/Cck+), and Somatosensory (Cck+) interneurons
Midnight blue (#7)	Cingulate (Layer 5 & 6), Somatosensory (Layer 5), and Basolateral amygdala pyramidal neurons
Orange (#8)	Cingulate (Cck+), Somatosensory (Cck+) and LGN interneurons
Pink (#9)	Cingulate (Layer 5 & 6), Somatosensory (Layer 5), Hippocampal, Basolateral amygdala, and Lateral amygdala pyramidal neurons
Purple (#10)	Cingulate (Layer 5 & 6), Somatosensory (Layer 5), and Basolateral amygdala pyramidal neurons
Red (#11)	LGN interneurons
Turquoise (#12)	Cingulate (Pvalb+) interneurons; Cingulate (Layer 5) and Somatosensory (Layer 5) pyramidal neurons
Yellow (#13)	Hippocampal (Sst+), Cingulate (Pvalb+) and LGN interneurons

A table of the different modules and their associated cell types. Each of the module eigengenes was inspected for those cell types that had high expression of the genes within the module. The module eigengene was compared to these patterns using an indicator vector (1-for types with high expression; 0-for types with low expression), and significance was determined using the Kruskal-Wallis test. All modules were significantly associated with these cell types ($p<0.004$).

Supplemental Table 4 - Comparison between module correspondence to strain and cell identity

Module	GIN	G42	G30	YFPH	C57/Bl6	Cell Identity
Black (#1)	0.4705	0.4828	0.0224	0.6206	0.1919	0.6822
Blue (#2)	0.1622	0.4723	0.4195	0.0227	0.1597	0.8011
Brown (#3)	0.4986	0.2720	0.1671	0.6533	0.1866	0.6901
Green (#4)	0.3945	0.4990	0.2356	0.7171	0.3509	0.9847
Green yellow (#5)	0.3497	0.4716	0.0034	0.6555	0.0052	0.8524
Light yellow (#6)	0.4420	0.1560	0.3650	0.6321	0.3000	0.9798
Midnight blue (#7)	0.4795	0.0550	0.3567	0.5587	0.3266	0.8022
Orange (#8)	0.2144	0.4195	0.4409	0.8306	0.1289	0.7442
Pink (#9)	0.7727	0.2745	0.0731	0.5762	0.3147	0.8416
Purple (#10)	0.5946	0.0220	0.1987	0.5571	0.1926	0.6975
Red (#11)	0.0227	0.6860	0.0208	0.4557	0.0846	0.9501
Turquoise (#12)	0.2228	0.0551	0.3960	0.4401	0.0959	0.7515
Yellow (#13)	0.4630	0.7067	0.2113	0.5676	0.2780	0.8975

This table displays the absolute value of the correlations between the module eigengene and genetic strain, as well as populations that had high expression of genes within the module, which is called "Cell Identity." In order to compare genetic strain and cell type expression to the module eigengenes, both genetic strain and populations with high expression were converted to indicator vectors (eg. 1 for specific strain or population with high expression and 0 for all other populations). These data suggest that with the exception of the orange module, most modules are best described the cell populations with high expression and not strain.

Supplemental Table 5 – Expression within the black (#1) module using the Allen Brain Atlas

Gene Symbol	Probe	k_{ME}	Hippocampus	Basolateral Amygdala	Lateral Amygdala
Plk2	1427005_at	0.92	X	X	X
Mast3	1435666_at	0.91	X	X	X
Nell2	1423561_at	0.88	X	X	X
	1422687_at	0.88			
Hn1	1448180_a_at	0.87	X	X	X
BC008163	1425328_at	0.87	X	X	X
Kpna4	1417974_at	0.87	X		
Spint2	1438968_x_at	0.86	X	X	X
Neo1	1434931_at	0.86	X	X	
Apeg1	1417305_at	0.86	X	X	
Spfh1	1424210_at	0.85	X	X	X
Gng10	1450649_at	0.85	X	X	
Ltk	1460300_a_at	0.84	X	X	
Gstp1	1449575_a_at	0.84	X	X	X
Hn1	1438988_x_at	0.83	X	X	X
Mmd	1423489_at	0.83	X	X	X
Baiap2	1451027_at	0.83	X	X	X
Elk1	1421897_at	0.82	X	X	X
Snrpg	1448358_s_at	0.82	X	X	X
1110033L15Rik	1453025_at	0.82			
Nap1l1	1420478_at	0.81	X	X	X
D2Bwg0891e	1451431_a_at	0.81	X	X	X
Rhou	1449027_at	0.81	X		
Hs2st1	1450729_at	0.81	X	X	X
Fancl	1423624_at	0.8			

This table displays all of the genes within the black module that were examined using the Allen Brain Atlas. The top twenty-five genes that had their maximum k_{ME} within the black module were selected, and the gene expression was visually inspected. The module eigengene was used to determine which regions to examine. An (X) within the table denotes presence of expression in that area and a blank cell denotes absence of expression.

Supplemental Table 6 – Expression within the brown (#3) module using the Allen Brain Atlas

Gene Symbol	Probe	k_{ME}	Layer V	Basolateral Amygdala
Tmod2	1431326_a_at	0.94	X	X
Rab2	1418622_at	0.93	X	X
Ywhaz	1448218_s_at	0.93	X	X
Capza2	1423058_at	0.92		
Dnaja2	1417183_at	0.91	X	X
Pcmt1	1431085_a_at	0.91	X	
Arf1	1420920_a_at	0.91	X	X
Eif4e	1450908_at	0.91	X	
Arl1	1451025_at	0.91	X	X
Ppp2cb	1421823_at	0.91	X	X
Pja1	1426449_a_at	0.91	X	X
Rpl5	1451077_at	0.9	X	X
Sept7	1454610_at	0.9	X	X
2310004l03Rik	1428698_at	0.89		
Vps24	1428165_at	0.89	X	X
Mat2b	1448196_at	0.89	X	X
Tde2	1415838_at	0.89	X	X
Ywhaq	1420828_s_at	0.89	X	X
Psarl	1433478_at	0.89		
Tgfb1i4	1454758_a_at	0.89	X	X
Hnrpab	1453849_s_at	0.88	X	X
Gabarapl1	1416418_at	0.88	X	X
Tspyl1	1415908_at	0.88	X	X
3930401K13Rik	1451994_s_at	0.88		
Ga17	1451076_s_at	0.88		X

This table displays all of the genes within the brown module that were examined using the Allen Brain Atlas. The top twenty-five genes that had their maximum k_{ME} within the black module were selected, and the gene expression was visually inspected. The module eigengene was used to determine which regions to examine. An (X) within the table denotes presence of expression in that area and a blank cell denotes absence of expression.

Supplemental Table 7 – Expression within the midnight blue (#7) module using the Allen Brain Atlas

Gene Symbol	Probe	k_{ME}	Layer V	Layer VI	Basolateral Amygdala
5330431N19Rik	1452603_at	0.91	X	X	X
Ppp1ca	1460165_at	0.91	X	X	X
Slc25a22	1452653_at	0.9	X	X	X
Synj2	1452344_at	0.9	X	X	X
Tomm34	1448345_at	0.89	X	X	X
Slc7a4	1426068_at	0.89	X	X	X
Ppp2r5c	1427003_at	0.88			
Ap3m2	1417527_at	0.88	X	X	X
Hk1	1437974_a_at	0.88	X	X	X
Pak1	1420980_at	0.87	X	X	X
Fbxo31	1417969_at	0.87	X	X	X
Atp6v1d	1416952_at	0.86	X	X	X
Dusp14	1431422_a_at	0.86	X	X	X
Cap2	1450910_at	0.86	X	X	X
Camk2b	1448676_at	0.86	X	X	X
Dph2l1	1418335_a_at	0.86			
Stx6	1450844_at	0.86	X	X	
Ssna1	1448643_at	0.86	X	X	X
Cyfip2	1449273_at	0.85	X	X	X
1110008P14Rik	1459890_s_at	0.85	X	X	X
Nudt3	1451575_a_at	0.85	X	X	X
Lin7b	1418683_at	0.85	X	X	X
Rab33a	1417529_at	0.85			
Myo18a	1451422_at	0.85	X	X	X
Fancl	1423624_at	0.8			

This table displays all of the genes within the brown module that were examined using the Allen Brain Atlas. The top twenty-five genes that had their maximum kME within the black module were selected, and the gene expression was visually inspected. The module eigengene was used to determine which regions to examine. An (X) within the table denotes presence of expression in that area and a blank cell denotes absence of expression.

Supplemental Table 8 - Correlation between module eigengenes and mean firing rate

	Correlation	P-value
	-0.66	0.00001
	0.62	0.00006
	0.59	0.00010
	-0.57	0.00027
	0.44	0.00665

	0.43	0.00855
	-0.35	0.03729
	0.27	0.11770

	0.13	0.43351
	-0.13	0.43502
	-0.13	0.44427

	-0.09	0.58894
	-0.03	0.87288

This table summarizes the correlation between the current clamp data and the first principal component of each module. The correlation of the first four modules (black, blue, pink, and yellow) is significant after correction for multiple comparisons ($p<0.004$).

Supplemental Table 9 - Comparison between modules and organelle proteome

Module	Nucleus	EE	ER	Golgi	Membrane	Mitochondria	RE	ER/Golgi vesicle
Black (#1)	0.37	2.28	0.71	2.12*	1.58	0.52	1.85	2.49*
Blue (#2)	0.63	0.65	0.81	0.69	0.72	3.43**	0.4	0.61
Brown (#3)	1.87*	2.4	1.8	2.29**	2.66**	0.88	3.31**	1.95*
Green (#4)	0.38	0.78	1.59	1.14	0.98	0.63	1.27	1.34
Green yellow (#5)	0.41	0	0.39	0.67	0	0.58	0	0.39
Light yellow (#6)	0	0	0.85	0.36	0.38	0.31	0.55	0.42
Midnight blue (#7)	0.23	0	1.53	0.93	0.78	0.48	0.85	1.09
Orange (#8)	1.15	0	0	0	1.64	0.27	1.2	0
Pink (#9)	0.43	0	0.41	0.53	0.37	0.3	0.13	0.41
Purple (#10)	1.12	1.15	1.79	0.91	1.27	1.31	1.4	1.07
Red (#11)	2.02*	0	0.19	0.17	0.52	0.29	0	0.19
Turquoise (#12)	1.04	1.83	1.14	1.46	0.64	2.41**	1.02	1.43
Yellow (#13)	0.84	1.73	1.08	0.69	0.72	0.99	1.06	0.81
Observed in network	77	25	80	94	90	109	123	80
Obtained from database	181	73	209	236	227	283	283	201

This table summarizes the comparison between the network defined modules and the proteomically defined organellar proteins. Each number corresponds to an observed/expected ratio. Out of the eight organelles examined, there were six that were significant without correction for multiple comparisons (*$p<0.05$) and of those four were significant after Bonferroni correction (**$p<0.004$). The last two rows describe how many proteins were in the network compared to the number obtained from the database. Abbreviations: EE - early endosome, ER - endoplasmic reticulum, RE - recycling endosome.

Supplemental Table 10 - Comparison between modules and the synaptic proteome

Module	Synaptosome	Post-synaptic density	Pre-synaptic fraction	Synaptic vesicles	Composite
Black (#1)	1.29	1.25	0.86	0	1.25
Blue (#2)	1.06	0.83	0.49	0	1.05
Brown (#3)	1.02	1.45*	1.82	0.92	1.12
Green (#4)	1.20	0.90	2.37*	0	1.16
Green yellow (#5)	0.63	0.12	0	0	0.48
Light yellow (#6)	0.80	0.99	2.05	0	0.79
Midnight blue (#7)	0.89	1.15	1.59	2.69	0.99
Orange (#8)	0.59	1.19	1.79	0	0.77
Pink (#9)	0.68	0.90	1.00	0	0.79
Purple (#10)	0.93	0.94	0	0	0.91
Red (#11)	0.82	0.57	0	0	0.71
Turquoise (#12)	1.74**	1.55*	1.04	3.52*	1.62**
Yellow (#13)	0.90	1.27	0.66	1.67	1.01
Total	553	273	33	13	728

This table summarizes the comparison between the network modules and the proteomically-characterized synaptic fractions. Each value corresponds to an observed/expected ratio. The composite represents all studies compiled into one list. The last row shows how many genes obtained from each study were present within the network. *$p<0.05$ & **$p<0.004$ (Bonferroni correction)